Journal of the Optical Society of America B
OPTICAL PHYSICS

Single-step creation of polarization gratings by scanning wave photopolymerization with unpolarized light [Invited]

Kyohei Hisano,[1] Megumi Ota,[1,2] Miho Aizawa,[1,2] Norihisa Akamatsu,[1,2] Christopher J. Barrett,[1,3] and Atsushi Shishido[1,2,*]

[1]Laboratory for Chemistry and Life Science, Institute of Innovative Research, Tokyo Institute of Technology, R1-12, 4259 Nagatsuta, Midori-ku, Yokohama 226-8503, Japan
[2]Department of Chemical Science and Engineering, School of Materials and Chemical Technology, Tokyo Institute of Technology, 2-12-1 Ookayama, Meguro-ku, Tokyo 152-8552, Japan
[3]Department of Chemistry, McGill University, 801 Sherbrooke Street West, Montreal, QC H3A 0B8, Canada
*Corresponding author: ashishid@res.titech.ac.jp

Received 17 December 2018; revised 23 January 2019; accepted 26 January 2019; posted 1 February 2019 (Doc. ID 355502); published 7 March 2019

Liquid crystalline materials with a cycloidal molecular orientation pattern are attractive for fabricating diffractive waveplates, diffracting incident light regardless of its polarization state into left- and/or right-circularly polarized light only in the +1st and/or −1st orders, applicable as next-generation optical devices. However, large-area high-speed processing of such molecular orientation is a challenge, since even state-of-the-art photoalignment methods require a precise spatial modulation of the polarization states of incident light, e.g., polarization holograms. Here, we propose and demonstrate that unpolarized light could easily generate cycloidal molecular orientation patterns over large areas in a single step merely by using our recently developed method of "scanning wave photopolymerization" with a simple optical setup. Importantly, the processing time for fabricating millimeter-scale films was significantly decreased to less than a few minutes. Detailed investigation revealed that the resultant film showed the desired diffraction behavior with a diffraction efficiency of 50%.

https://doi.org/10.1364/JOSAB.36.00D112

1. INTRODUCTION

Diffractive waveplates (DWs) are polarization gratings, few-micrometers-thick films based on liquid crystals (LCs) with precise molecular orientation patterns producing extremely high diffraction efficiencies. Rational design of DWs is key to developing some of the greatest emerging technologies in the field of next-generation photonics [1–17]. One of the greatest benefits is that in using several stacked DW films, one can replace massive optical systems for manipulating light, which are typically composed of large and complex arrays of optical elements such as lenses, prisms, polarization converters, etc. The optical properties of DWs are governed by the orientation patterns of LCs because the patterned birefringence (Δn) has the ability to spatially modulate the phase of light. As the most simple example of such modulation, a one-dimensionally (1D) aligned LC can act as a linearly polarized light converter, termed a half-wave plate, where retardation ($R = \Delta n \cdot d$; d is the thickness of the medium) is matched exactly to $\lambda/2$ (λ: wavelength of incident light). In the same manner, the inscription of more complexed two-dimensional (2D) orientation patterns of LCs allows one to realize versatile geometrical phase modulations, producing various optical functionalities (e.g., lenses, optical vortex generators, beam steering, etc.) [10,13,16]. Specifically, LC films with a cycloidal molecular orientation pattern are known as "cycloidal diffractive waveplates (CDWs)" and have especially attracted a great deal of attention. Such films with orientation patterns meeting the half-wave plate condition diffract the incident light only into the +1st and −1st orders with the polarization state of left- and right-circular polarization, respectively (Fig. 1) [1–11]. Thus, CDWs have the potential to open windows for the application of next-generation projection displays.

Thanks to the recent development of control methods over molecular orientation, such complex 2D orientation patterns of LCs have been readily achieved. The most advanced procedure is a "surface photoalignment control" technology [18–23]. Generally, one can control LC orientation through photoreactions of a thin film coated over a substrate surface. The coating films contain photoresponsive dyes such as azobenzene or cinnamate moieties, so that the irradiation of a film with uniform polarized light results in an orientation of dyes perpendicular to the polarization direction. The LCs over the film surface also spontaneously align along the direction of dyes. Therefore,

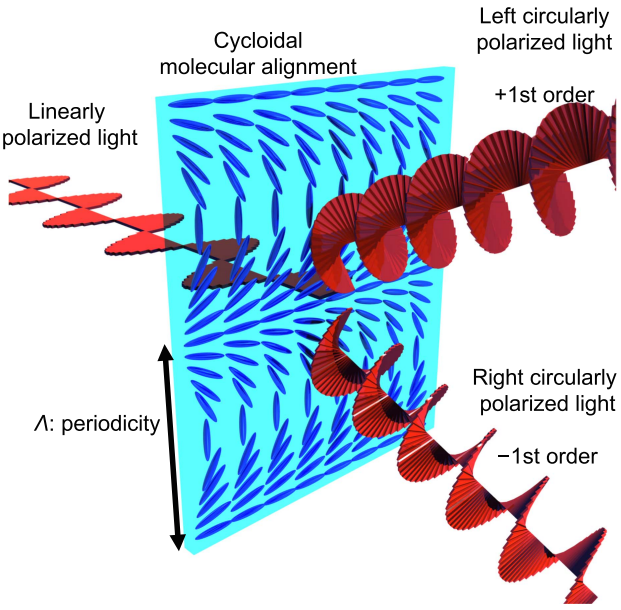

Fig. 1. Schematic illustration of the light diffraction behavior of a film with a cycloidal molecular orientation pattern. A linearly polarized light beam passing through the medium is diffracted into the +1st and −1st orders with left- and right-circularly polarized light, respectively. A left-circularly polarized light is diffracted into the −1st order light with right handedness, and vice versa. Λ donates the physical periodicity of the cycloidal orientation. Blue ellipses represent liquid crystals.

the spatial modulation of the polarization state of incident light can generate 2D molecular orientation patterns. To control the spatial polarization states, state-of-the-art technologies have been proposed with the use of specially designed optical setups with numerous optical elements: computer-generated holograms, plasmonic photomasks, spatial light modulators, and polarization holograms [1,24–27]. For the fabrication of CWDs, the polarization holograms are mostly used where one merely exposes a photoresponsive film to two circularly polarized light beams with inversed handedness overlapped orthogonally at the selected position. This method has a great advantage of high spatial resolution (less than tens of micrometers) with highly precise cycloidal orientation patterns; thus, recently novel CDWs with a diffraction efficiency over 95% and/or with achromatic features ($\Delta\lambda > 200$ nm) have been realized [13,28]. However, there remain scientific challenges in increasing processability, producing CDWs over large areas, and avoiding the complex optical setup currently requiring the interference of two circularly polarized beams. Photoalignment technologies have achieved the creation of large-area CDWs by photoalignment of a dye-containing layer and subsequent photopolymerization of aligned reactive mesogens on a photoalignment layer [11,16]. This method requires spatial modulation of the polarization direction in each pixel, which increases process time to obtain large-area CDWs.

Here we report the single-step creation of CDWs over large areas even without polarized light, using our recently developed method of scanning wave photopolymerization (SWaP) [29–31]. As we have already reported, SWaP offers a principal advantage over conventional photoalignment methods using photoreaction of dyes under polarized light. In SWaP, photopolymerization with a focused, guided unpolarized light generates a localized polymerization reaction, which directly generates a mass flow of molecules perpendicular to the edge of the irradiated regions and/or parallel to the light scanning direction. Then, this mass flow aligns molecules along the flow direction, and SWaP thus enables one to inscribe arbitrary 2D orientation patterns (various DWs) over large areas in a single step merely by spatiotemporal scanning of a patterned light during photopolymerization, without the need for any dyes, surface treatments, or further processing steps. Since such patterned light can be generated just from unpolarized light passing through a photomask, SWaP has a great advantage of simplicity in optical setup, offering a facile incorporation into existing industrial photoproduction lines. As a first step, we demonstrated the inscription of cycloidal molecular orientation patterns by SWaP by a single-step irradiation with an optical pattern of the 1D scanning of light with a periodically arranged rod-shaped pattern for less than 3 min. The resultant polymer film adopted a periodicity in the orientation pattern of ∼30 μm over an area of 4.4 mm × 2.5 mm. Detailed investigation of the optical functionalities by using a probe laser beam revealed that the resultant film performed successfully as a CDW with a diffractive efficiency of 50%. Taking into account that the SWaP could generate the orientation pattern merely by 1D scanning of light with the periodically arranged rod-shaped pattern, this process could be applicable in a roll-to-roll production line for large-area fabrication, with the potential of generating a film with an essentially unlimited size.

2. MATERIALS AND FABRICATION PROCEDURE

The fabrication process and the photopolymerizable materials for creating a LC polymeric film with a cycloidal molecular orientation pattern were the same as previously reported for the inscription of 2D molecular orientation patterns by SWaP [30]. First, as depicted in Fig. 2, a glass cell was prepared by adhering two cleaned glass substrates without any surface treatment, and the cell thickness was set to c.a. 3 μm by using glue including silica spacers (diameter of 2 μm). Then, a solid-state sample, composed of a photopolymerizable anisotropic monomer, a crosslinker, and a commercially available UV-photoinitiator, was injected into the glass cell on a hot stage at its isotropic clearing temperature (150°C). After annealing for 2 min, the cell was cooled down to the photopolymerization temperature, which was the LC temperature of the resultant polymer (100°C). Next, SWaP was conducted as per the following steps. To precisely design microscopic and/or complex 2D patterns of molecular orientation, we developed an optical setup, termed POM-DLP that is a digital light processor (DLP) connected to a polarized optical microscope (POM). In POM-DLP, the LED light source (λ_{max}, 372 nm) was equipped with a digital micromirror device (DMD; Texas Instruments, DLP3010; number of pixels, 1280 × 720; size of each pixel, 5.4 μm), as a UV light source with a dynamic photomask. In addition, POM-DLP has a POM, and thus we could conduct *in situ* observation of photopolymerization. This provides us with information about the relationship between the resultant molecular orientation and the irradiated optical pattern, which allows easy optimization of polymerization conditions. The other benefit of the POM-DLP setup is that the POM can be fitted with

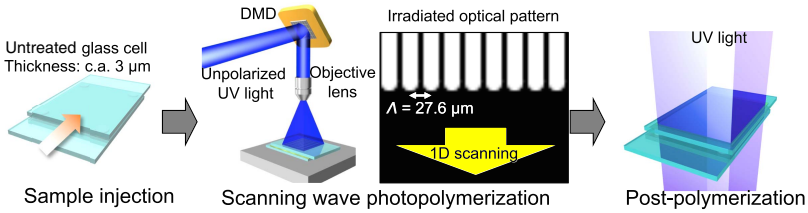

Fig. 2. Schematic illustrations of the fabrication of a polymeric film by using SWaP. The irradiated optical pattern that has the periodically arranged rod shape: Λ, 27.6 μm; width of each rod, 20.7 μm) was 1D scanned at the rate of 15 μm/s (Visualization 1). The size of the whole area irradiated by light was 4.4 mm × 2.5 mm. The yellow arrow represents the light scanning direction.

a variety of different objective lenses whose magnification typically ranges from ×4 to ×10 to ×20 by focusing the incident light, leading to good control of the resolution of the irradiation pattern merely by changing objective lenses. By using a beam profiler (OPHIR-SPIRICON, SP620) located at the stage of POM, the size of each pixel irradiated at the sample stage with a ×4 objective lens was found to be 3.45 μm × 3.45 μm. We irradiated samples set on a stage of the POM with an arbitrary desired UV pattern designed with Adobe Illustrator software. Then, we irradiated the whole cell to complete polymerization and fixed the resultant molecular orientation patterns. Finally, the resultant polymer film was rapidly cooled down below its glass transition temperature in liquid nitrogen.

3. DESIGN OF THE OPTICAL PATTERN

As described above, a cycloidal molecular orientation pattern has the potential to function as a diffraction element. These films can diffract unpolarized or linearly polarized light as left- and right-circularly polarized light only into the +1st and −1st orders, respectively, when the medium meets the half-wave plate condition. Such diffractive behavior can also be observed when circularly polarized light is illuminated normal to the medium and generates diffraction light of the +1st or −1st order depending on its handedness. To manifest such optical functionality, patterns are required to be fabricated with a size below tens of micrometers in pitch. Theoretically, the diffraction angle α_{theory} can be expressed by the following equation:

$$\alpha_{\text{theory}} = \arcsin[2R/\Lambda], \quad \textbf{(1)}$$

where R denotes the retardation of the LC film and Λ denotes the physical periodicity of the cycloidal molecular orientation patterns. According to Eq. (1), the diffraction angle becomes ∼1.3° when the wavelength of the incident laser is 633 nm (He–Ne laser), and the film should have both a retardation of 317 nm (half-wave plate condition) and a periodicity of ∼30 μm.

4. RESULTS AND DISCUSSION

The photopolymerization conditions were optimized to generate uniform, precise cycloidal molecular orientation patterns by SWaP in the sample by using a designed optical pattern of 1D scanning of light with the periodically arranged rod-shaped pattern (Fig. 2 and Visualization 1). In this study, we used a POM-DLP with an ×4 objective lens. The process time for polymerizing the film of 4.4 mm × 2.5 mm was less than 3 min. According to our previous report [30], the SWaP can generate molecular orientation with a birefringence of ∼0.1, and here we fabricated and used a glass cell with a 3.52 μm thickness, calculated from the data of the UV–vis transmission spectra, to achieve a retardation of ∼317 nm. Figure 3(A) shows the POM observation of a resultant film polymerized with UV light at an intensity of 2.4 mW/cm^2. The POM image clearly showed that the film had a grating structure with the same physical periodicity as the irradiated optical pattern. The bright fringes were observed along the grating vector, which was perpendicular to the light scanning direction. This indicates that the periodically arranged rod-shaped pattern caused the periodic molecular orientation as well as the periodic change in refractive index. The observation with POM with a tint plate (R = 530 nm) revealed that the induced periodic molecular orientation pattern had a physical periodicity of ∼27.6 μm, as designed and expected. Furthermore, we observed the film under a POM equipped with both an interference filter (λ = 546 nm) and a Berek compensator, and thus the retardation of the film was found to be 332 nm. To further investigate the exact direction of the molecular orientation, we observed the film under polarizers and analyzers that were rotated simultaneously every 30°, maintaining the light scanning direction at θ = 0° as shown in Fig. 3(B). The bright fringes gradually shifted along the grating vector (perpendicular to the light scanning direction) in accordance with the rotation of the polarizer and analyzer, and finally the initial pattern was observed at θ = 180°. Considering that the dark areas in the fringes can be observed only when the molecular orientation direction is parallel or perpendicular to the polarizer or analyzer, it would be a cycloidal molecular orientation pattern along the light scanning direction that was induced as shown in Fig. 3(B-iii). To quantitatively evaluate the recorded molecular orientation pattern in the resultant polymer film, we performed a calculation of the orientation angles in a transverse position (pitch) of the fabricated film. Although the ideal cycloidal molecular orientation pattern has the linear variation of the angle with the distance in every pitch, the resultant pattern was in a subtly different manner (Fig. 4). Considering that the molecular orientation generated by SWaP is ruled by the optical pattern of the irradiated light, further optimization of the optical pattern enables one to generate a truly cycloidal molecular orientation.

According to the proposed mechanism of SWaP, the reason why the inscription of the optical pattern resulted in cycloidal orientation patterns, even with unpolarized light patterned by a very simple optical setup, is readily rationalized. Before initiating

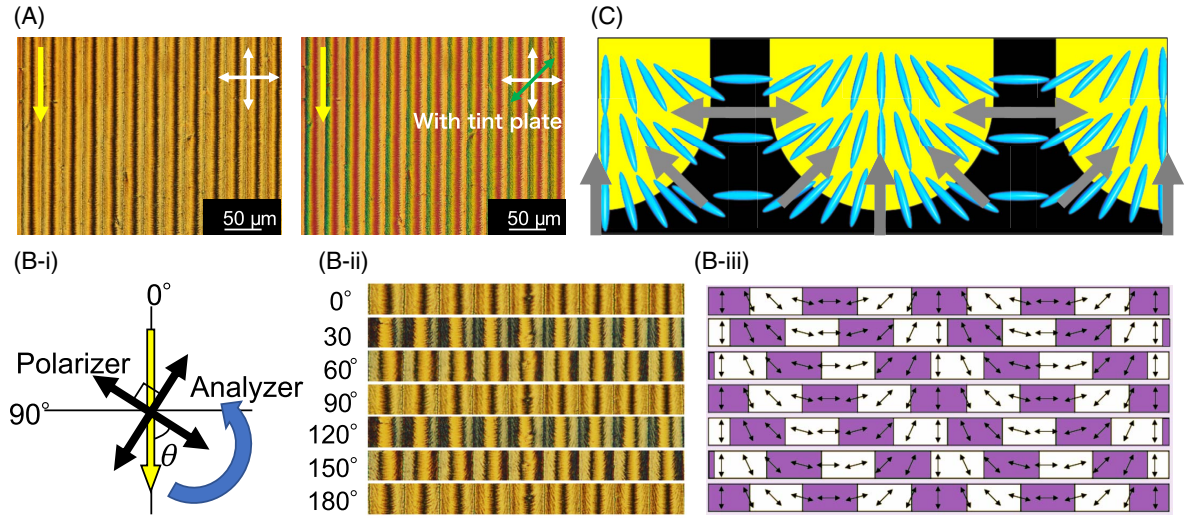

Fig. 3. (A) POM images of a film under crossed polarizers without (left) and with a tint plate (right). White and green arrows show the direction of polarizers and the optical axis of the tint plate, respectively. Yellow arrows depict the light scanning direction. (B) Observation of the molecular orientation under the polarizer and analyzer simultaneously rotated. (i) Schematic illustration of the setup. (ii) POM images observed as a function of the rotation angle (θ) of the polarizer and analyzer. (iii) Molecular orientation pattern directed by SWaP. White and purple areas represent the bright and dark areas in (ii), respectively. (C) A schematic illustration of a cycloidal molecular orientation (denoted by blue ellipses) and the mass flow direction during SWaP (denoted by grey arrows). Yellow and black regions represent the light irradiated and unirradiated regions, respectively.

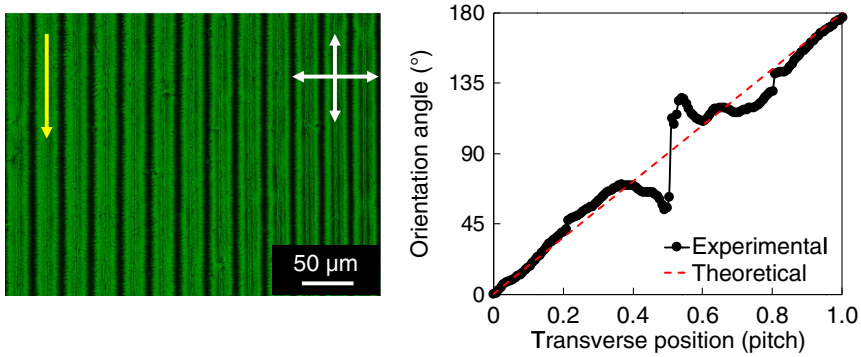

Fig. 4. Investigation of the molecular orientation angles as a function of a transverse position (pitch) of the fabricated CDW. POM observation with a 546 nm light source (left), the calculated orientation angle in a transverse position (right, solid black line), and the theoretical angle of a cycloidal molecular orientation (right, dashed red line). White crossed arrows show the direction of the polarizers, and the yellow arrow depicts the light scanning direction. Here the angles were simply calculated by the equation $T(\%) = \sin^2(\frac{\pi R}{\lambda})\sin^2 2\theta$, where λ represents the wavelength of light (546 nm) used for the observation with a polarized optical microscope, R represents the retardation of the fabricated film (332 nm) evaluated with a Berek compensator, and T at each wavelength represents the transmittance of light passing through both a film and the crossed polarizers of the POM. The transmittance was calculated by using the image analyzing software (Image J).

photopolymerization, the monomers lie along random orientations at their isotropic temperature. The exposure of monomers to unpolarized UV light on a selected region (periodically arranged rod-shaped pattern) generates polymers and creates a spatial gradient of chemical potential that triggers a mass flow arising from molecular diffusion. This mass flow takes place along the vector direction perpendicular to the boundary between polymerized and unpolymerized regions and/or parallel to the light scanning direction. Since the mass flow has the ability to align the molecules along the flow direction, the irradiated optical pattern enables one to direct the molecular orientation in a cycloidal manner as schematically depicted in Fig. 3(C). Note that the periodicity of the cycloidal molecular orientation pattern depends on the period of the irradiated optical pattern; thus, in principle, we could fabricate various CDWs by modifying the spatiotemporal patterns of the incident light. Furthermore, this proposed mechanism ensures that the generation of a cycloidal molecular orientation by SWaP can be expanded to as large as desired by combining with a roll-to-roll photoproduction facility. Of particular appeal here is the feasibility of high-speed processing of the cycloidal orientation pattern over large areas. Compared with conventional photoalignment methods, which require more than a few minutes for inscribing patterns over one square millimeter, the inscription time in the present report is comparably short; it took ~3 min to fabricate a film with 4.4 mm × 2.5 mm areas by using a 1D beam scanning at a rate of 15 μm/s. In theory,

however, SWaP has the potential to create CDWs with millimeter sizes in just a millisecond, since the scanning rate of SWaP has now been shown to be able to be increased up to 13.7 mm/s, based on our previous report for generating a uniform 1D orientation [30].

To evaluate the optical functionality of the resultant polymer film, we employed an optical setup equipped with a He–Ne laser ($\lambda = 633$ nm) to meet the half-wave plate condition as shown in Fig. 5(A). A laser beam was incident on the film, passing through a polarizer and a quarter-wave plate to obtain a circularly polarized light (CPL) beam with right or left handedness depending on the angle of the quarter-wave plate. The transmitted and diffracted beams from the film were observed on a screen, and the 2D light intensity profile was monitored with a CCD camera. We evaluated the diffraction angle (α_{eval}) by using the following equation:

$$\alpha_{eval} = \arctan(D/l). \quad (2)$$

The film clearly showed a selective diffraction when the CPL was normally incident on the film, and left- and right-circularly polarized diffracted light was observed on the −1st and +1st orders, respectively (Fig. 5(B)). The diffraction angle was observed to be 1.36°, and this value matched well with the theoretical value calculated by Eq. (1), which was predicted to be 1.38°. On the other hand, when the incident light was linearly polarized, both the −1st- and +1st-order diffracted beams were observed. Furthermore, to evaluate the polarization state of the diffracted laser beams, an additional quarter-wave plate was placed after the film so that we could convert a circularly polarized light into linearly polarized light. By setting a polarizer after the quarter-wave plate, we analyzed the polarization direction of the output beam. The intensity of diffractive light passing through both the quarter-wave plate and polarizer became almost zero when these optical elements were inserted at an appropriate angle. This clearly indicates that the +1st- and −1st-order diffracted beams are left- and right-circularly polarized, respectively. The incident beams were converted into the circularly polarized light with the inversed handedness, and the resultant film was found to successfully act as a CDW.

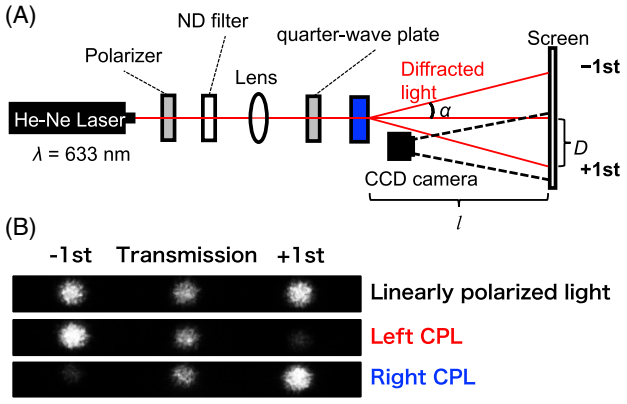

Fig. 5. (A) Side view of the optical setup for evaluation of optical functionality of a film with a cycloidal molecular orientation pattern. The diffracted light on a screen was detected with a CCD camera. The diffracted angle α was calculated using the equation depicted in Eq. (2), where D represents the distance between the transmission and the diffracted (±1st) beam and l represents the distance between the film and the screen. (B) Representative 2D light intensity profiles of the output beam (top, linearly polarized; middle, left-circularly polarized; bottom, right-circularly polarized light), passing through the film with cycloidal molecular orientation with a retardation of 332 nm, detected with a CCD camera.

To quantitatively evaluate the diffraction behavior, the intensities of the incident, transmitted, and diffracted beams were individually measured with an optical power meter. We calculated the light diffraction efficiency (η), which was defined as the ratio of the first-order diffraction beam intensity (I_1) passing through the film to the incident beam intensity (I_0) as expressed by the following equation:

$$\eta = I_1/I_0 \times 100(\%). \quad (3)$$

First, we used a linearly polarized beam, which was normally incident to the film. The light passing through the film was observed as the zeroth transmission (7.7%), −1st- (30.7%), and +1st- (29.6%) order diffraction as shown in Fig. 5(B). When the left-circularly polarized light (Left CPL) was normally incident on the film, the −1st-order diffraction showed the highest diffraction efficiency of 55.3%, and that of the +1st order became the smallest relative intensity of 5.3%. Likewise, when the right-circularly polarized light (Right CPL) was incident, the +1st-order diffraction showed the highest diffraction efficiency of 55.8%, and the −1st-order diffraction efficiency decreased to 4.0%. The results are summarized in Table 1. In order to evaluate the losses of the incident light that was not diffracted into the −1 and/or +1 orders, we measured the power of both the diffraction into the higher orders and Fresnel back-reflections. As a result, the incident light was converted into the higher-order diffraction (∼10%) with the reflections (∼7%). These results indicated that ∼15% of the incident light might be scattered away. In addition, the ratio between −1st versus +1st when the incident light was linearly polarized, left-circularly polarized, or right-circularly polarized was calculated to be 50:52, 10:1, and 1:14, respectively. The high scattering ratio and the low contrast ratio between −1st versus +1st with the incident light of CPL can be attributed to the inhomogeneity of the recorded molecular orientation pattern in the film compared with the truly cycloidal molecular orientation such as

1. orientational defects of LCs with the size of a few micrometers might randomly be located in a periodical pitches of the cycloidal molecular orientation;
2. the angle variation with a transverse position of the recorded molecular orientation was different from the ideal linear variation of the cycloidal molecular orientation as explained above.

Table 1. Diffraction Efficiency of the Output Beam[a]

	Diffraction Efficiency (%)		
Incident Light	−1st Order	Transmission	+1st Order
Linearly polarized light	29.6	7.7	30.7
Left CPL	55.3	6.7	5.3
Right CPL	4.0	6.4	55.8

[a]The efficiency of the output beam was calculated by averaging the values in the three different points.

This does not, however, suggest a fundamental limitation of the CDW fabricated by SWaP, since these both issues could likely be overcome by further optimizing SWaP conditions. We thus believe that the polarization-selective diffraction film with a large-area cycloidal molecular orientation pattern generated by SWaP in a single step has great potential to be applicable to next-generation optical device fabrication.

5. CONCLUSION

First, we demonstrated the single-step and high-speed processing of a polarization grating by employing our recently developed method of "SWaP" with unpolarized light patterned through a very simple optical setup; there was no need to use any lasers, polarizers, or interference systems. The resultant LC polymer film had a cycloidal molecular orientation pattern over a large area and acted as a successful CDW that diffracted and converted an incident beam into right- and/or left-circularly polarized beams. Considering that the key to generating a cycloidal molecular orientation pattern is the 1D scanning of light with a periodically arranged rod-shaped pattern during photopolymerization, SWaP provides one with the opportunity to create an extraordinarily large-area film merely by introducing a roll-to-roll process into existing fabrication production lines. Furthermore, we believe that the general ability to pattern arbitrarily via SWaP represents a new and exciting platform for inscribing such 2D molecular orientation patterns quickly, easily, and inexpensively over large areas, enabling one to readily industrially fabricate not only CDWs but also various types of DWs with optical functionalities such as lenses, optical vortex converting, beam steering, etc.

Funding. Precursory Research for Embryonic Science and Technology (PRESTO) (JPMJPR14K9); Japan Science and Technology Agency (JST); Japan Society for the Promotion of Science (JSPS) (JP17H05250, JP18H05422, JP18H05984, JP18J15144, JP18K14297); Core Research for Evolutional Science and Technology (CREST) (JPMJCR18I4).

Acknowledgment. This work was supported by the Precursory Research for Embryonic Science and Technology (PRESTO) program, "Molecular Technology and Creation of New Functions," and the Japan Science and Technology Agency (JST). This work was supported by the Japan Society for the Promotion of Science (JSPS) KAKENHI in Scientific Research on Innovative Areas "Photosynergetics." This work was supported by JSPS KAKENHI in Scientific Research on Innovative Areas, "Molecular Engine: Design of Autonomous Functions through Energy Conversion." This work was supported by the Core Research for Evolutional Science and Technology (CREST) program, "Creation of Innovative Core Technologies for Nano-enabled Thermal Management" and JST. This work was supported by JSPS KAKENHI. This work was performed under the Research Program for CORE Labs and the Research Program for Next Generation Young Scientists of "Network Joint Research Center for Materials and Devices." The Tokyo Institute of Technology is thanked for sabbatical visit funding for Barrett in 2017 to the Shishido Labs, as Visiting Adjunct Professor.

REFERENCES

1. R. H. Berg, S. Hvilsted, and P. S. Ramanujam, "Peptide oligomers for holographic data storage," Nature **383**, 505–508 (1996).
2. Z. Bomzon, G. Biener, V. Kleiner, and E. Hasman, "Space-variant Pancharatnam-Berry phase optical elements with computer-generated subwavelength gratings," Opt. Lett. **27**, 1141–1143 (2002).
3. H. Sarkissian, S. V. Serak, N. V. Tabiryan, L. B. Glebov, V. Rotar, and B. Ya. Zeldovich, "Polarization-controlled switching between diffraction orders in transverse-periodically aligned nematic liquid crystals," Opt. Lett. **31**, 2248–2250 (2006).
4. L. Marrucci, C. Manzo, and D. Paparo, "Pancharatnam-Berry phase optical elements for wave front shaping in the visible domain: switchable helical mode generation," Appl. Phys. Lett. **88**, 221102 (2006).
5. C. Provenzano, P. Pagliusi, and G. Cipparrone, "Highly efficient liquid crystal based diffraction grating induced by polarization holograms at the aligning surfaces," Appl. Phys. Lett. **89**, 121105 (2006).
6. M. Ishiguro, D. Sato, A. Shishido, and T. Ikeda, "Bragg-type polarization gratings formed in thick polymer films containing azobenzene and tolane moieties," Langmuir **23**, 332–338 (2007).
7. A. Shishido, M. Ishiguro, and T. Ikeda, "Circular arrangement of mesogens induced in Bragg-type polarization holograms of thick azobenzene copolymer films with a tolane moiety," Chem. Lett. **36**, 1146–1147 (2007).
8. L. Nikolova and P. S. Ramanujam, *Polarization Holography* (Cambridge University, 2009).
9. S. R. Nersisyan, N. V. Tabiryan, D. M. Steeves, and B. R. Kimball, "Optical axis gratings in liquid crystals and their use for polarization insensitive optical switching," J. Nonlinear Opt. Phys. **18**, 1–47 (2009).
10. S. R. Nersisyan, N. V. Tabiryan, D. M. Steeves, and B. R. Kimball, "The promise of diffractive waveplates," Opt. Photon. News **21**(3), 40–45 (2010).
11. A. Shishido, "Rewritable holograms based on azobenzene-containing liquid-crystalline polymers," Polym. J. **42**, 525–533 (2010).
12. S. R. Nersisyan, N. V. Tabiryan, D. M. Steeves, and E. Serabyn, "Improving vector vortex waveplates for high-contrast coronagraphy," Opt. Express **21**, 8205–8213 (2013).
13. J. Kim, Y. Li, M. N. Miskiewicz, C. Oh, M. W. Kudenov, and M. J. Escuti, "Fabrication of ideal geometric-phase holograms with arbitrary wavefronts," Optica **2**, 958–964 (2015).
14. N. V. Tabiryan, S. V. Serak, S. R. Nersisyan, D. E. Roberts, B. Y. Zeldovich, D. M. Steeves, and B. R. Kimball, "Broadband waveplate lenses," Opt. Express **24**, 7091–7102 (2016).
15. J. Kobashi, H. Yoshida, and M. Ozaki, "Planar optics with patterned chiral liquid crystals," Nat. Photonics **10**, 389–392 (2016).
16. S. V. Serak, D. E. Roberts, J.-Y. Hwang, S. R. Nersisyan, N. V. Tabiryan, T. J. Bunning, D. M. Steeves, and B. R. Kimball, "Diffractive waveplate arrays," J. Opt. Soc. Am. B **34**, B56–B63 (2017).
17. Y. H. Lee, G. Tan, T. Zhan, Y. Weng, G. Liu, F. Gou, F. Peng, N. V. Tabiryan, S. Gauza, and S. T. Wu, "Recent progress in Pancharatnam–Berry phase optical elements and the applications for virtual/augmented realities," Optical Data Processing and Storage **3**, 79–88 (2017).
18. O. Yaroshchuk and Y. Reznikov, "Photoalignment of liquid crystals: basics and current trends," J. Mater. Chem. **22**, 286–300 (2012).
19. T. Seki, S. Nagano, and M. Hara, "Versatility of photoalignment techniques: from nematics to a wide range of functional materials," Polymer **54**, 6053–6072 (2013).
20. V. G. Chigrinov, V. M. Kozenkov, and H.-S. Kwok, *Photoalignment of Liquid Crystalline Materials: Physics and Applications* (Wiley, 2008).
21. A. Priimagi, C. J. Barrett, and A. Shishido, "Recent twists in photoactuation and photoalignment control," J. Mater. Chem. C **2**, 7155–7162 (2014).
22. T. Seki, "Light-directed alignment, surface morphing and related processes: recent trends," J. Mater. Chem. C **4**, 7895–7910 (2016).
23. T. Seki, "New strategies and implications for the photoalignment of liquid crystalline polymers," Polym. J. **46**, 751–768 (2014).

24. L. De Sio, D. Roberts, Z. Liao, S. Nersisyan, O. Uskova, L. Wickboldt, N. Tabiryan, D. Steeves, and B. Kimball, "Digital polarization holography advancing geometrical phase optics," Opt. Express **24**, 18297–18306 (2016).
25. Y. Guo, M. Jiang, C. Peng, K. Sun, O. Yaroshchuk, O. Lavrentovich, and Q.-H. Wei, "High-resolution and high-throughput plasmonic photopatterning of complex molecular orientations in liquid crystals," Adv. Mater. **28**, 2353–2358 (2016).
26. A. Ogiwara and T. Hirokari, "Formation of anisotropic diffraction gratings in a polymer-dispersed liquid crystal by polarization modulation using a spatial light modulator," Appl. Opt. **47**, 3015–3022 (2008).
27. L. Nikolova and T. Todorov, "Diffraction efficiency and selectivity of polarization holographic recording," Opt. Acta **31**, 579–588 (1984).
28. C. Oh and M. J. Escuti, "Achromatic diffraction from polarization gratings with high efficiency," Opt. Lett. **33**, 2287–2289 (2008).
29. K. Hisano, Y. Kurata, M. Aizawa, M. Ishizu, T. Sasaki, and A. Shishido, "Alignment layer-free molecular ordering induced by masked photopolymerization with non-polarized light," Appl. Phys. Express **9**, 072601 (2016).
30. K. Hisano, M. Aizawa, M. Ishizu, Y. Kurata, W. Nakano, N. Akamatsu, C. J. Barrett, and A. Shishido, "Scanning wave photopolymerization enables dye-free alignment patterning of liquid crystals," Sci. Adv. **3**, e1701610 (2017).
31. M. Aizawa, K. Hisano, M. Ishizu, N. Akamatsu, C. J. Barrett, and A. Shishido, "Unpolarized light-induced alignment of azobenzene by scanning wave photopolymerization," Polym. J. **50**, 753–759 (2018).